Chapter 8

A Rain Estimation System Based on Electromagnetic Propagation Models and DVB-S Opportunistic Sensors

Daniele Caviglia, Matteo Pastorino,
Andrea Randazzo and Andrea Caridi

Additional information is available at the end of the chapter

http://dx.doi.org/10.5772/66726

Abstract

Weather conditions have in general huge impact on the global economy, in particular on agriculture, industry, transport, and so forth. In recent years, also the occurrences of rapid and localized heavy rainfall in complex topographic areas became more frequent, possibly due to global warming. These facts cause injuries and deaths, and an accurate and early alert system is required to warn people and operators. In this chapter, we describe a real-time and low-cost system for precipitation detection, aimed at collecting additional data with respect to those obtainable from traditional sensors. Such a system is based on the opportunistic usage of satellite digital video broadcasting (DVB-S) microwave signals and estimates the rain intensity from the detected attenuation. Our system proved to accurately obtain results comparable with rain gauges located in the experimentation area, with much tighter spatial and temporal scales than traditional schemes.

Keywords: rainfall estimation, nowcasting, antennas, electromagnetic propagation, electronic circuits

1. Introduction

In several countries around the world, the occurrence of flash flood events is notably increasing with more extensive damages. Usually, flash flooding is a result of heavy localized rainfall, such as that from slow moving intense thunderstorms. Consequently, in the last few years, there has been an increasing interest in developing techniques aimed at regularly monitoring the amount of rainfall [1–7].

Besides the well-known weather prediction networks aimed at providing information on the expected precipitation, the monitoring of rainfalls during the events is now considered of

paramount importance for the civil protection. The most used apparatuses for rainfall measurement are based on rain gauges, wheatear radars, radiometers, and global positioning system (GPS) systems. Rain gauges measure the quantity of rain fallen into a small bucket in a predefined time interval, usually in the range of 10–15 minutes. Therefore, they are not generally suitable for real-time monitoring of the atmospheric phenomenon, especially when dealing with thunderstorms that may occur over small basins, with a size of a few square kilometres, and consequently a lag time in the order of half an hour, or even less.

Weather surveillance radars (WSR) [8] exploit the reflection of the electromagnetic waves when impinging on hydrometeors in order to create maps of inspected regions, which are generally quite large (over 100 km in radius). In this case, too, the data are usually acquired every 10–15 minutes. The main problem of WSR is the high installation and maintenance cost, which does not allow to deploy a large number of measurement stations. X-band radars have also been proposed for weather monitoring [9, 10]. In this case, however, the useful range is limited (usually less than 60 km), requiring to create networks of interconnected systems in order to monitor a large area. GPS-based systems employ the microwave signal transmitted for positioning and navigation purposes in order to estimate the rainfall [11]. In fact, the time delay of the signal received by the receivers at earth (tropospheric delay) depends upon the dielectric properties of the atmosphere, and consequently, upon its water content [12]. However, it is worth noting that the quantity that can be extracted from the analysis of the tropospheric delay is just the precipitable water and not the actual rain at earth.

Recently, the rapid growth of mobile communications resulted in a global spread of wireless networks operating in the microwave band. Such networks can be used in an opportunistic way for environmental characterization [13]. In particular, the attenuation level of the measured signal can be used to estimate the intensity of the rain. This attenuation is caused by the phenomena of absorption and "scattering" of the electromagnetic field due to the water droplets in air, which are most significant for frequencies above 10 GHz (i.e., when the wavelength of the electromagnetic waves assumes the values of the same order of magnitude of the diameter of the drops). In this framework, the use of terrestrial links between mobile communication base stations, usually working at frequencies in the K or Ka bands, has been proposed in the literature for estimating the rainfall near the earth surface [14–17]. The main drawback of this method consists in the fact that such microwave links are mainly deployed in urban areas, while the hills and mountains that collect waterfall and produce flood events are scarcely covered. A second problem deals with the ownership of the infrastructure and propagation data by telecom operators, which requires their involvement in the process.

Given this situation, the opportunistic usage of attenuation data of the microwave links from geostationary satellites has been proposed recently [1–4]. In this chapter, we will describe a rain monitoring system based on the measurement of the electromagnetic radiation received by standard antennas used by commercial satellite digital video broadcasting (DVB-S) decoders. The developed apparatus employs a logarithmic amplifier/detector to convert the antenna received power into a voltage, which is then acquired by an analog-to-digital converter and transmitted to a central node via a wired or wireless link. The data are stored in a database and processed in order to estimate the rain rate over the area of interest. A mathematical model

http://dx.doi.org/10.5772/66726

based on antennas and propagation concepts is used to describe the relationship between the rain intensity and the measured values. In particular, the well-assessed ITU model described in [18] is employed for relating the specific attenuation along the path to the rain rate.

The chapter is organized as follows: in Section 2, the electromagnetic waves propagation and attenuation model is briefly reviewed. In Section 3, the developed rainfall estimation system is described. In Section 4, some experimental results are provided and discussed. Finally, conclusions are outlined in Section 5.

2. Mathematical formulation

From an electromagnetic point of view, the formulation of the approach is based on the propagation and attenuation of the electromagnetic waves transmitted by a commercial satellite for broadcasting services. In the far field of the transmitting antenna, the field is locally a plane wave, i.e.,

$$\mathbf{E}(\mathbf{r}) = E_p(\mathbf{r})e^{-jk\hat{\mathbf{k}}\cdot\mathbf{r}}\hat{\mathbf{p}} \tag{1}$$

$$\mathbf{H}(\mathbf{r}) = \frac{1}{\eta}E_p(\mathbf{r})e^{-jk\hat{\mathbf{k}}\cdot\mathbf{r}}\hat{\mathbf{k}}\times\hat{\mathbf{p}} \tag{2}$$

where $\mathbf{r}$ is the position vector, $\hat{\mathbf{p}}$ and $\hat{\mathbf{k}}$ are unit vectors denoting the polarization and direction of propagation, $k = \beta - j\alpha$ is the complex propagation constant (its real part is the phase constant and the imaginary part is the attenuation constant, whose unit is m^{-1}), E_p is the field amplitude, and η is the intrinsic impedance of the propagation medium. The power density of the wave is given by the Pointing vector, i.e.,

$$\mathbf{S}(\mathbf{r}) = \frac{1}{2}\mathbf{E}(\mathbf{r})\times\mathbf{H}^*(\mathbf{r}) = \frac{1}{2\eta}\left|E_p\right|^2 e^{-2\alpha\hat{\mathbf{k}}\cdot\mathbf{r}}\hat{\mathbf{k}} = S_k(\mathbf{r})\hat{\mathbf{k}} \tag{3}$$

When the attenuation due to atmospheric gases, multipath, and other effects can be neglected, the available power at the receiving antenna (located at position $\mathbf{r}_{RX}$) can be expressed as

$$P_L = A_{\text{eff}}\,S_k(\mathbf{r}_{RX}) \tag{4}$$

where A_{eff} denotes the effective area of the receiving antenna. Since

$$A_{\text{eff}} = e_{\text{pol}}\,e_{\text{load}}\frac{\lambda^2}{4\pi}G_{RX} \tag{5}$$

where G_{RX} is the gain of the receiving antenna and e_{pol} and e_{load} are the polarization and the load matching efficiencies, it results

$$P_L = \frac{\lambda^2}{4\pi}G_{RX}\,e_{\text{pol}}\,e_{\text{load}}\,S_d(\mathbf{r}_{RX}) \tag{6}$$

There are two conditions to be compared. In the first case, we assume that no rain is present. In this case, we denote the received power as P_L^0. When rainfall is present, there is an extra

attenuation that contributes to the imaginary part of the propagation constant. Therefore, we can write the attenuation due to rain as

$$L_{\text{rain}} = \frac{P_L^0}{P_L} = e^{2\alpha_{\text{rain}} l_{\text{rain}}} \tag{7}$$

where l_{rain} is the length of the path traveled by the plane wave interested by the rain. Since the rain originates at a height h_{rain} above the sea (as schematically shown in **Figure 1**), the length of the path interested by the rain is given by

$$l_{\text{rain}} = \frac{h_{\text{rain}} - h_{RX}}{\sin\theta_{\text{el}}} \tag{8}$$

where h_{RX} is the altitude of the receiving antenna and θ_{el} is its elevation angle. The rain height mainly depends upon the geographical location of the receiving antenna and can be obtained from weather services or by using the mean values provided in the ITU recommendation P.839 [19].

By expressing the attenuation L_{rain} in dB (L_{rain}^{dB}) and l_{rain} in kilometers ($l_{\text{rain}}^{\text{km}}$), we obtain

$$L_{\text{rain}}^{\text{dB}} = P_L^{0\ \text{dBm}} - P_L^{\text{dBm}} = 10\log e^{2\alpha_{\text{rain}} l_{\text{rain}}} = 20\,\alpha_{\text{rain}}\, l_{\text{rain}} \log e = \alpha_{\text{rain}}^{dB/\text{km}}\, l_{\text{rain}}^{\text{km}} \tag{9}$$

where $\alpha_{\text{rain}}^{\text{dB/km}} = 0.02\,\alpha_{\text{rain}} \log e$ is the specific attenuation and the superscript dBm indicates that the quantities are expressed in decibel (referred to 1 mW).

According to ITU recommendation P.838 [18], which assumes that the specific attenuation is constant over the whole length interested by the rainfall, the attenuation per unit length, $\alpha_{\text{rain}}^{\text{Km}}$ [dB/km], is related to the rain rate r (mm/h) by the following equation

$$\alpha_{\text{rain}}^{\text{dB/Km}} = B\, r^A \tag{10}$$

where B and A are two coefficients that depends upon the frequency and the polarization of the electromagnetic wave. Normally, by using the ITU model, it is only possible to retrieve a global information about the overall rain rate along such path.

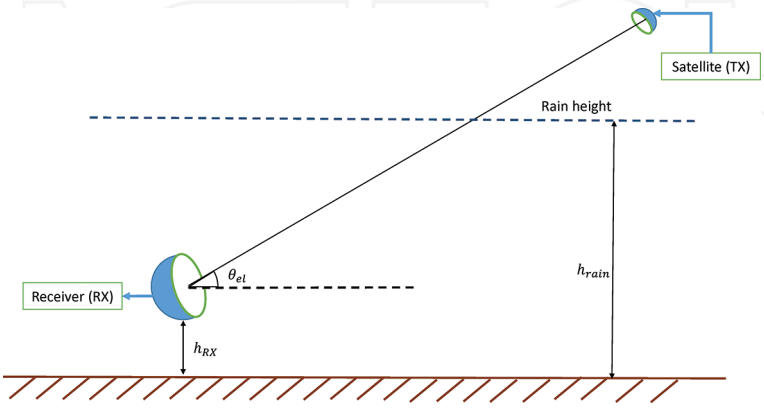

Figure 1. Schematic representation of the considered configuration.

http://dx.doi.org/10.5772/66726

By combining the model (10) and the link budget (9), the following equation is obtained

$$P_L^{\mathrm{dBm}} = P_L^{0\ \mathrm{dBm}} - B\, l_{\mathrm{rain}}^{\mathrm{km}}\, r^A = P_L^{0\ \mathrm{dBm}} - B\, l_{\mathrm{rain}}^{\mathrm{km}} \left(\frac{h_{\mathrm{rain}} - h_{RX}}{\sin\theta_{el}}\right)^A \tag{11}$$

which must be inverted in order to find the rain rate r starting from the received power. The superscript km in Eq. (11) indicates that the heights are expressed in kilometers. Consequently, it results that the rain rate can be estimated as

$$r = \left[\frac{P_L^{0\ \mathrm{dBm}} - P_L^{\mathrm{dBm}}}{B\left(h_{\mathrm{rain}}^{\mathrm{km}} - h_{RX}^{\mathrm{km}}\right)} \sin\theta_{el}\right]^{\frac{1}{A}} \tag{12}$$

It is worth noting that, in order to solve Eq. (12), the knowledge of the reference power P_L^0 (i.e., the received power in absence of rainfalls) is required. Such quantity can be estimated from historical data.

3. System description

The considered system exploits the information contained in the signal at the output of a low noise block (LNB), commonly used in the receiving chain of a consumer DVB-S set. In particular, the power level is measured by an ad-hoc designed sensor and the output of such sensor is then "inverted" in order to estimate the rainfall. The block diagram of the proposed measurement system is shown in **Figure 2**. Its main parts consist in a sensing board, a microcontroller unit, and a network interface.

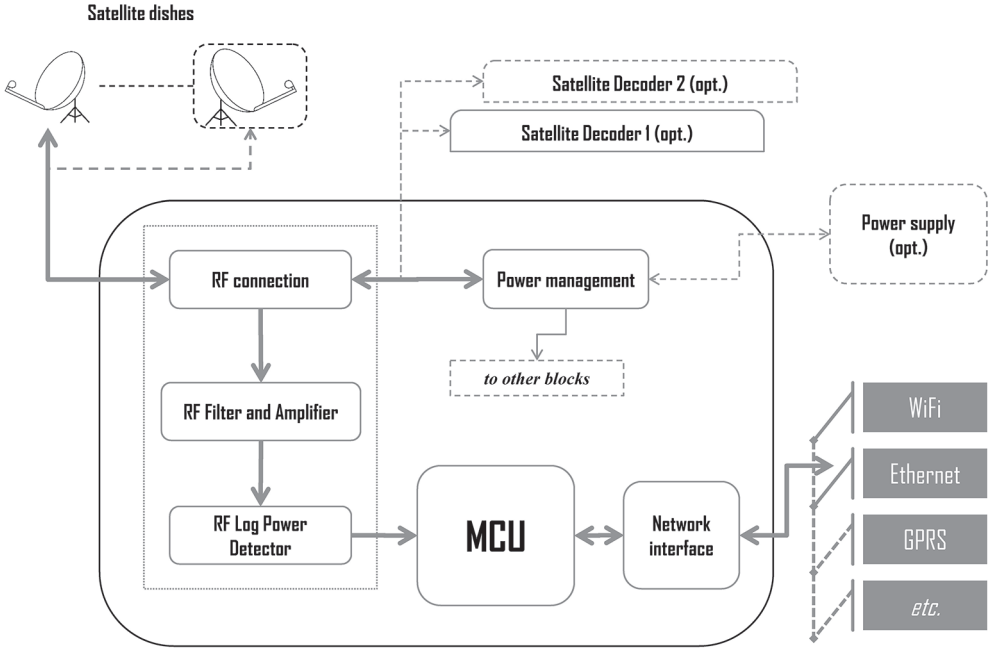

Figure 2. DVB-S power detector module.

The data acquisition module is connected to one or more receiving antennas for standard DVB-S television equipped with universal LNBs. Such devices, whose general block diagram is schematically shown in **Figure 3**, perform a first amplification and a down conversion of the signals received by the antennas. In particular, the electromagnetic waves propagating from the satellite to the user antenna have frequencies in the range of 10.7–12.75 GHz. In the LNB, such frequency band is divided into two subbands of approximately 1 GHz width each (low and high), which are downconverted in the range of 950–2150 MHz by mixing the received signal with a local reference signal having the suitable frequency (9.75 and 10.6 GHz for the low and high bands, respectively). The selection of the band forwarded to the decoder is performed by superimposing to the supply voltage a 22 kHz tone with amplitude of 0.5 V (if the tone is present, the high band is selected, otherwise the low one is used). In this way, it is possible to connect the LNB to the decoder (which in practical installation could be located at a distance of several tens of meters) with a low-cost cable and a reasonable attenuation (usage of the original frequencies would have required a much more expensive guiding structure). In order to increase the link capacity, two polarizations, horizontal and vertical, are also used (in our implementation we do not consider circularly polarized systems). The polarization selection is carried out by a control circuit in the LNB on the basis of the DC supply voltage (13 and 18 V for vertical and horizontal polarizations, respectively). It is worth noting that such a kind of LNB does not perform any automatic gain control (AGC) and thus preserves proportionality between the amplitudes of the received signal and the one forwarded to the decoder. Consequently, the power at the output of the LNB module can be modeled as $P_D = G_{conv} P_L$, where P_L is power received by the antenna and G_{conv} is the conversion gain of the downconverter, including all the possible gains of the eventually present amplifiers and the cable losses.

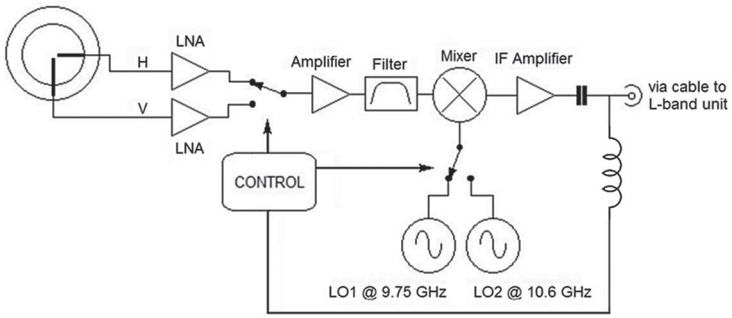

Figure 3. Universal low noise block (LNB) diagram.

The signal coming from the LNB is applied to the logarithmic power detector module via a directional coupler ("RF connection"), a filter and an amplifier (see **Figure 2**). The directional coupler performs two operations. First, it conveys the signal to a possible decoder without a significant attenuation, allowing the use of the antennas employed for usual TV operations with no inconvenience for the user. On the other direction, the power supply 13/18 V and the possible 22 kHz tone are transferred from the decoder to the LNB. The system can be operated

http://dx.doi.org/10.5772/66726

also without any decoder: in such a case, a dedicated power supply module is needed. At the same time, the directional coupler also directs part of the signal to the measurement electronics. The extracted signal, properly amplified and filtered, is processed by a logarithmic power detector, which integrates the signal power over the entire band 950–2050 MHz. In particular, the voltage at the output of the RF detector is related to the input power over a wide range by means of the following linear relationship

$$P_D^{\mathrm{dBm}} = c_1 V_{\mathrm{out}}^{\mu\mathrm{V}} + c_2 \tag{13}$$

where c_1 and c_2 are two parameters depending on the frequency range and on the used converter. The subscripts dBm and μV denote the measurement units. In the developed prototype, an analog device AD8314 detector [20] has been used, for which at the frequencies of interest, it results $c_1 = 50\ \mu\mathrm{V/dBm}$ and $c_2 = -53\ \mathrm{dBm}$.

The voltage signal is finally converted in digital format by using an analog-digital converter available in the microcontroller unit (MCU). The possible presence of the 22 kHz tone as well as the value of the supply voltage is detected, too. Such data, indicating band and polarization of the received signal, can be used to adapt the inversion algorithm parameters to best estimate the intensity of the precipitation.

The firmware in the MCU also performs the following functions:

- sample the signals at predefined intervals;
- carry out a preprocessing of the acquired data (e.g., average the measurements over a predefined number of acquisitions);
- package the data in a suitably defined format;
- send the data to the central server via the "network interface."

In the present implementation, the measurement hardware samples the detected power level each second, averages the readings and delivers the data packet with an interval of 1 minute. It is worth noting that we decided to take advantage of the whole L-band signal supplied by the LNB, with the aim at averaging over the set of all available transponders the variation of transmitted power. This operation has also the advantage to avoid the adoption of a receiver, thus resulting in a cost reduction, which is particularly useful in the case of realization of a network of sensors arranged densely on a vast territory. A further consequence is to take advantage of the signals coming from the three satellites of the constellation, which exhibit different oscillations around their nominal position: in this way, the obtained reference level appears to be quite stable, and consequently the rain-no-rain detection algorithm is facilitated. A different choice has been reported in Ref. [2], where channels at specific frequencies have been used.

The required power supply for the sensor module is derived opportunistically from the DC supply voltage (13/18 V) present on the cable, in the same way according to which the LNB is powered. This is achieved via an appropriate "power management" unit equipped with a buck converter, able to provide the voltage needed to power both the signal detection

module and the network interface. In addition, proper low-dropout regulators are employed, to improve the quality of the supply voltage, both in terms of stability and of noise content. Finally, it is worth noting that the "network interface" can be connected to different modules (such as LAN or Wi-Fi network, and also GPRS or LPWAN), depending on the connection possibilities available in the various sites.

A picture of the developed RF sensing board is shown in **Figure 4** [the two F connectors provide connectivity toward the decoder (left) and to the LNB (right)].

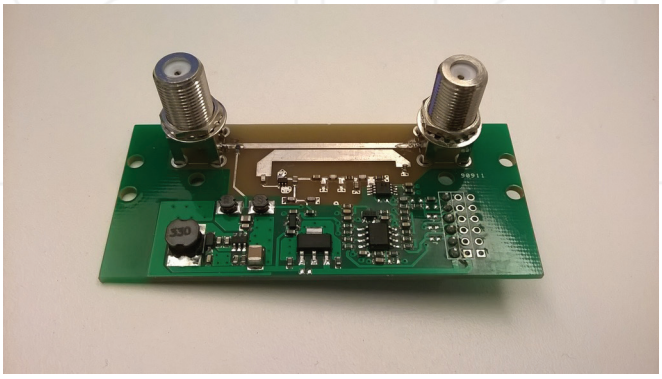

Figure 4. RF power detection board.

4. Experimental results

The developed system has been validated by using a test site located at the Department of Electrical, Electronic, and Telecommunication Engineering, and Naval Architecture (DITEN) of the University of Genoa. The antenna, which is installed at coordinates (44.4033° N, 8.959° E) and at a height $h_{\text{dish}} = 60$ m above the sea level, is pointed toward the Eutelsat "Hot Bird" commercial broadcasting satellite constellation at 13.0°E. The low-band, vertical polarization combination was chosen. An example of the output of the RF detector, related to a period of 36 hours, is shown in **Figure 5**. In the same figure, the corresponding received power is also reported, obtained by applying the transformation in Eq. (13). As it can be seen, the received power is almost constant and equal to about −18.5 dBm (in the considered period) when there is no rain (the left part of the graph, for an approximately 5 hours long interval). The occurrence of rainfall yields an attenuation in the range of 2–5 dB (depending on the rain intensity).

The data in **Figure 5** have been used to test the rain rate estimation approach described in Section 2. The parameters a and b have been chosen according to the ITU recommendation P.838-3 [18]. In particular, the following values have been used: $A = 1.16$; $B = 0.017$. The elevation angle of the dish antenna, for the considered satellite, is equal to $\theta_{\text{el}} = 38.7°$. The rain heigth $h_{\text{rain}_{\text{ITU}}}$ has been computed by using the empirical model defined in the ITU recommendation P.839-4 [19], i.e.,

http://dx.doi.org/10.5772/66726

$$h_{\text{rain}_{\text{km}}} = h_{0_{\text{km}}} + 0.36 = 3.27 \text{ km} \quad (14)$$

where h_0 is the zero isotherm height, which depends upon the geographical position of the test site and can be estimated by using the mean tabulated values provided by ITU. The length of the part of the slant path interested by the rain, computed by using Eq. (8), is equal to $l_{\text{rain}} = 5.23$ km. The reference power level $P_L^{0\ \text{dBm}}$ has been estimated from the historical data set. In particular, it has been found by searching the "flat" parts of the time series (after a noise filtering) and by averaging the corresponding measured power values. The obtained values, for the considered test case, is $P_L^{0\ \text{dBm}} = -18.66$ dBm. The rainfall intensity is shown in **Figure 6**. In particular, such graph reports the quantity, $R = r\delta t$, where r is the rain rate estimated by using Eq. (12).

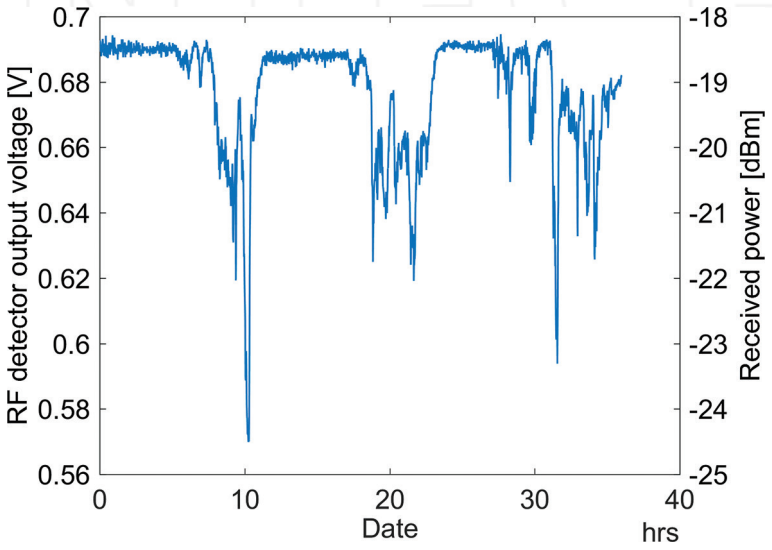

Figure 5. Output voltage of the RF detector and corresponding measured power.

In order to evaluate the correctness of the obtained results, they have been compared with the measurements of a standard rain gauge, made available by the Department of Civil, Chemical and Environmental Engineering (DICCA) of the University of Genoa [21]. Such instrument is located near the test site and provides the rainfall over periods of 30 minutes. Consequently, the estimated rain quantity has been integrated over the same period in order to obtain comparable values (denoted as R_{30}). The obtained results are shown in **Figure 7**. As it can be seen, there is a quite good agreement between the measured and the reference values. The small differences can be motivated by two facts. First, the rain gauge is not exactly below the path antenna-satellite. Moreover, it provides information about the rain in a single point, whereas the proposed estimation system gives an integral measure of the overall rain along the propagation path.

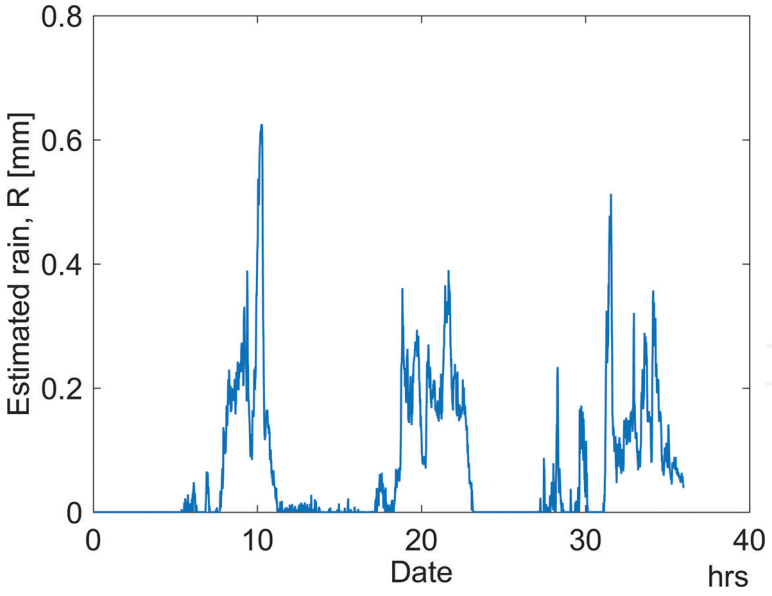

Figure 6. Estimated rainfall.

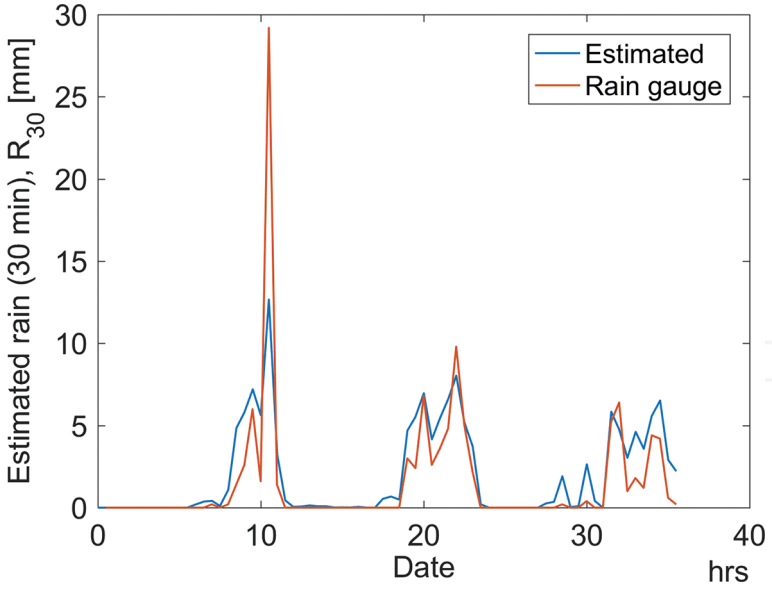

Figure 7. Estimation of accumulated rainfall in 30-minute intervals, and comparison with the measurements provided by a rain gauge.

http://dx.doi.org/10.5772/66726

5. Conclusions

In this chapter, a novel rain monitoring system has been proposed. The approach is based on the measurement of the electromagnetic radiation by using standard antennas adopted by commercial DVB-S decoders. It is based mathematically on the receiving properties of the antenna and the inversion of the ITU model for rain precipitations. In the chapter, both hardware and software have been described.

Experimental results have also been reported. They concerned comparison with data obtained by standard rain gauge. Although, preliminary, these results confirm the possibility of calculating with good accuracy the rainfall over the electromagnetic path, allowing the potential of a very largely distributed low-cost measurement network. Further developments will be devoted at exploring the possibility of combining multiple data collected by several separate rain monitoring apparatuses of this kind.

Author details

Daniele Caviglia[1,2], Matteo Pastorino[1]*, Andrea Randazzo[1,2] and Andrea Caridi[2]

*Address all correspondence to: pastorino@dibe.unige.it

1 Department of Electrical, Electronic, Telecommunications Engineering and Naval Architecture (DITEN), University of Genoa, Genova, Italy

2 Artys Srl, Piazza della Vittoria, Genova, Italy

References

[1] B. Federici, G. L. Gragnani, G. parodi, A. Randazzo, D. Caviglia, M. Pastorino, D. Sguerso, A. Caridi, and C. Montecucco. System and method for monitoring a territory. EU Patent EP2688223A1. 22-01-2014.

[2] L. Barthès and C. Mallet. Rainfall measurement from the opportunistic use of an Earth–space link in the Ku band. Atmospheric Measurement Techniques. 2013;**6**(8):2181–2193.

[3] K. S. Choi, J. H. Kim, and D. S. Ahn. System and method for integrally collecting rainfall attenuation and rainfall intensity data in satellite system. US Patent US20130130618A1. 23-05-2013.

[4] L. Brocca, C. Massari, L. Ciabatta, W. Wagner, and A. Stoffelen. Remote sensing of terrestrial rainfall from Ku-band scatterometers. IEEE Journal of Selected Topics in Applied Earth Observations and Remote Sensing. 2016;**9**(1):533–539.

[5] H. Chen and V. Chandrasekar. Estimation of light rainfall using Ku-band dual-polarization radar. IEEE Transactions on Geoscience and Remote Sensing. 2015;**53**(9):5197–5208.

[6] J. Shi, C. Xu, J. Guo, and Y. Gao. Real-time GPS precise point positioning-based precipitable water vapor estimation for rainfall monitoring and forecasting. IEEE Transactions on Geoscience and Remote Sensing. 2015;**53**(6):3452–3459.

[7] V. Pastoriza, F. Machado, P. Marino, and F. P. Fontan. Nowcasting of the spatiotemporal rain field evolution for radio propagation studies. IEEE Transactions on Antennas and Propagation. 2013;**61**(6):3312–3320.

[8] M. I. Skolnik. Radar Handbook. 3rd edition. New York: McGraw-Hill; 2008.

[9] M. Gabella, R. Notarpietro, S. Turso, and G. Perona. Simulated and measured X-band radar reflectivity of land in mountainous terrain using a fan-beam antenna. International Journal of Remote Sensing. 2008;**29**(10):2869–2878.

[10] S. Turso, S. Paolella, M. Gabella, and G. Perona. MicroRadarNet: A network of weather micro radars for the identification of local high resolution precipitation patterns. Atmospheric Research. 2013;**119**:81–96.

[11] M. Bevis, S. Businger, T. A. Herring, C. Rocken, R. A. Anthes, and R. H. Ware. GPS meteorology: Remote sensing of atmospheric water vapor using the global positioning system. Journal of Geophysical Research. 1992;**97**(D14):15787.

[12] E. D. Kaplan and C. Hegarty, Eds. Understanding GPS: Principles and Applications. 2nd ed. Boston: Artech House; 2006.

[13] H. Messer. Environmental monitoring by wireless communication networks. Science. 2006;**312**(5774):713–713.

[14] H. Leijnse, R. Uijlenhoet, and J. N. M. Stricker. Rainfall measurement using radio links from cellular communication networks. Water Resources Research. 2007;**43**(3):1-6.

[15] H. Messer, A. Zinevich, and P. Alpert. Environmental sensor networks using existing wireless communication systems for rainfall and wind velocity measurements. IEEE Instrumentation & Measurement Magazine. 2012;**15**(2):32–38.

[16] O. Goldshtein, H. Messer, and A. Zinevich. Rain rate estimation using measurements from commercial telecommunications links. IEEE Transactions on Signal Processing. 2009;**57**(4):1616–1625.

[17] A. Zinevich, P. Alpert, and H. Messer. Estimation of rainfall fields using commercial microwave communication networks of variable density. Advances in Water Resources. 2008;**31**(11):1470–1480.

[18] Recommendation ITU-R P.838-3, "Specific attenuation model for rain for use in prediction methods", International Telecommunication Union, 2005

[19] Recommendation ITU-R P.839-4, "Rain height model for prediction methods", International Telecommunication Union. 2013.

[20] Analog Devices. 100 MHz to 2.7 GHz, 45 dB RF Detector/Controller. AD8314 Datasheet. 2006.

[21] DICCA Weather Station. [Online]. Available: http://www.dicca.unige.it/meteo/.